Supplementary Material (ESI) for *CrystEngComm*
This journal is © The Royal Society of Chemistry

Three Photochromic Materials based on POMs and Viologens for UV Probing, Visual Detection of Metal Ions and Amine Detecting

Xi Xu, Mengle Yang*, Qinghai Lu, Shuang Yu, Shufang Ma, Aixiang Tian, Jun Ying*

Table S1. Selected bond lengths (Å) and angles (°) of compounds **1–3.**

Compound **1**

Cu(1) – Cl(1)	2.290(5)	Cu(1) – N(4)	2.016(13)
Cu(1) – Cl(1)^1	2.660(4)	Cu(1) – N(7)	2.031(13)
Cl(1) – Cu(1) – Cl(1)^1	88.38(15)	N(4) – Cu(1) – N(1)	87.2(5)
N(4) – Cu(1) – Cl(1)	175.5(4)	N(4) – Cu(1) – N(7)	92.8(5)
N(4) – Cu(1) – Cl(1)^1	95.3(4)	N(7) – Cu(1) – Cl(1)^1	97.3(4)

Symmetry codes: #1 1-X, 1-Y, 1-Z #2 1-X, 2-Y, 1-Z #3 1-X, 3-Y, -Z #4 2-X, 1-Y, 1-Z

Compound **2**

Mo(4) – Mo(1)	3.2052(7)	C(3) – C(6)	1.482(8)
Mo(4) – O(3)	1.687(4)	N(1) – C(1)	1.314(10)
Mo(3) – Mo(4) – Mo(1)	90.199(18)	C(8) – N(2) – C(10)	120.1(6)
O(3) – Mo(4) – O(13)	100.83(18)	C(10) – N(2) – C(11)	119.5(6)
O(8) – Mo(3) – Mo(4)	133.93(17)	C(4) – C(3) – C(2)	117.8(6)

Symmetry codes: #1 -X, -Y, 1-Z

Compound **3**

Mo(11) – O(33)	1.790(6)	N(5) – C(42)	1.303(12)
Mo(2) – O(22)	2.129(6)	C(10) – C(11)	1.504(14)
O(35) – Mo(11) – O(33)	109.0(3)	N(5) – C(41) – C(40)	120.2(9)
O(2) – Mo(5) – Mo(8)	124.65(17)	C(7) – C(10) – C(9)	118.2(11)
O(17) – Mo(1) – O(15)	145.5(2)	N(1) – C(19) – C(18)	117.9 (12)

Symmetry codes: #1 -X, 3-Y, 3-Z #2 1-X, 3-Y, 4-Z #3 -X, 2-Y, 2-Z

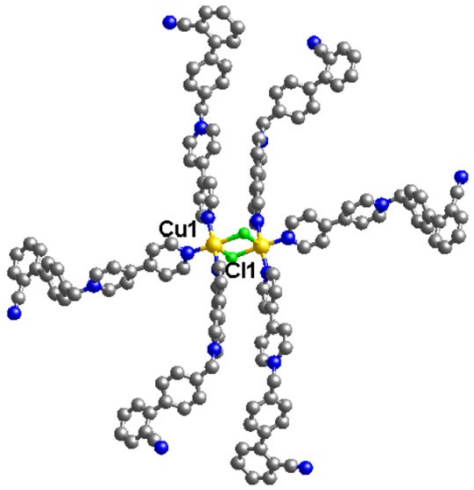

Fig. S1. The bi-nuclear Cu cluster constructed by six Cbybpy ligands of compound **1**.

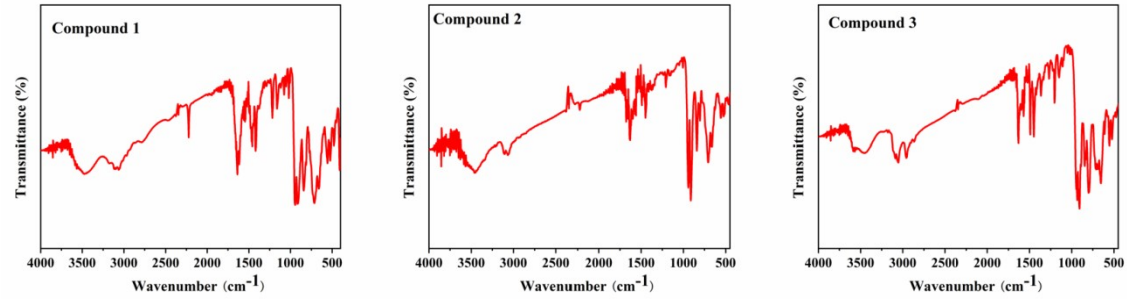

Fig. S2. The IR spectra of compounds **1–3**.

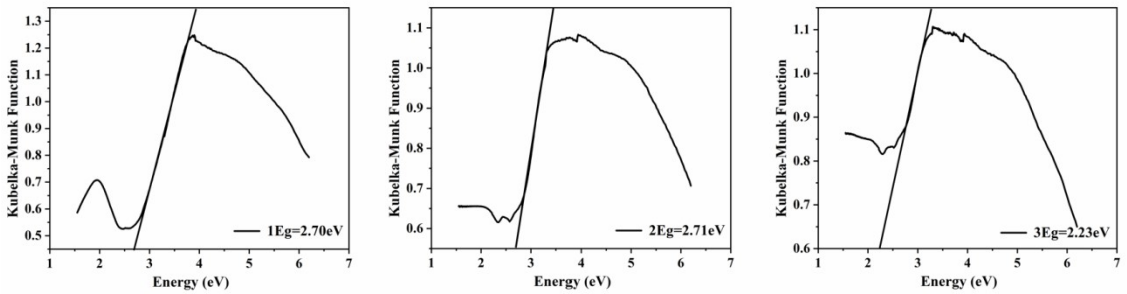

Fig. S3. The solid-state optical diffuse-reflectance spectra of compounds **1–3**.

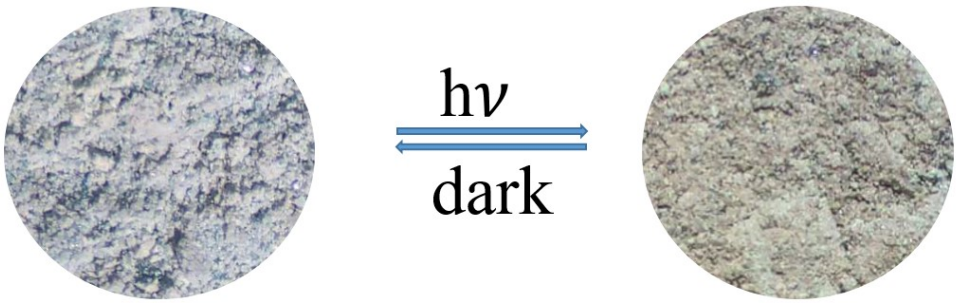

Fig. S4. Color change of compound **1** before and after photochromism.

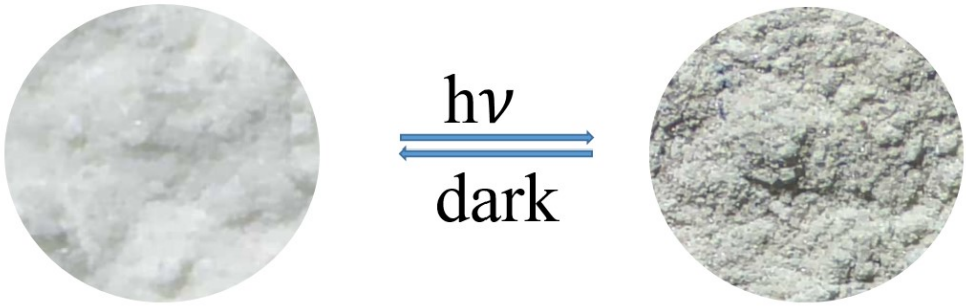

Fig. S5. Color change of compound **2** before and after photochromism.

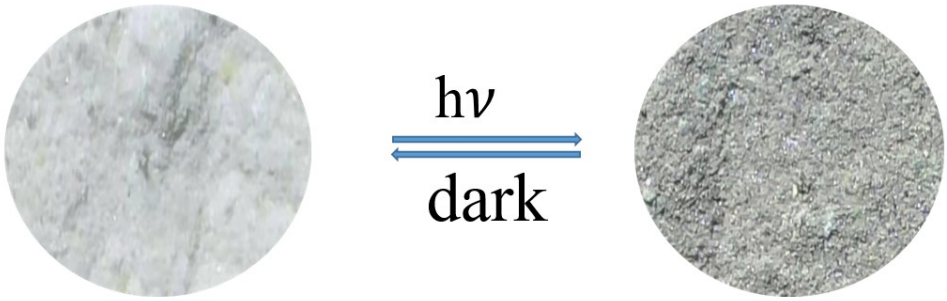

Fig. S6. Color change of compound **3** before and after photochromism.

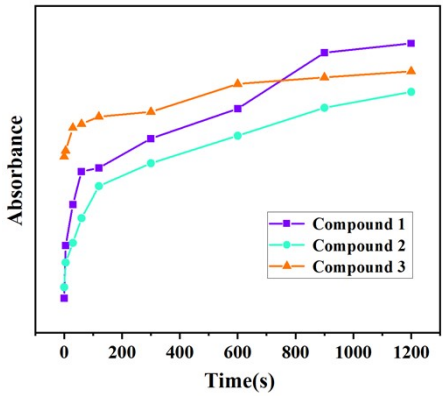

Fig. S7. The plots of absorption changes at 475 nm for **1**, 505 nm for **2**, 514 nm for **3** with irradiation time vs. UV irradiance.

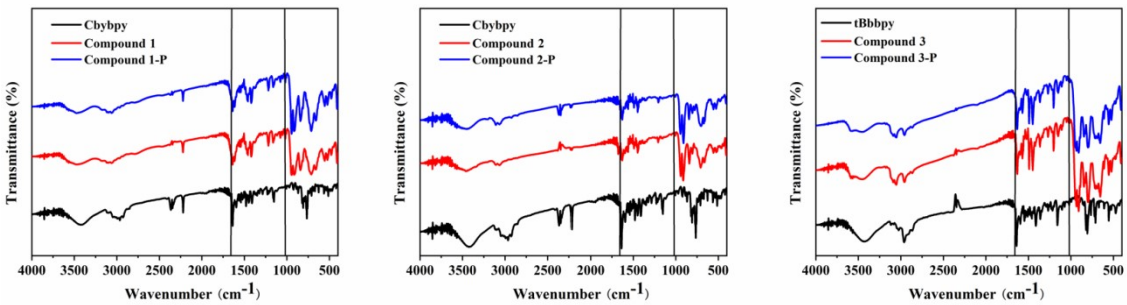

Fig. S8. The IR spectra of Cbybpy, tBbbpy, compounds **1–3** (before irradiation) and compounds **1**-P, **2**-P, **3**-P (after irradiation).

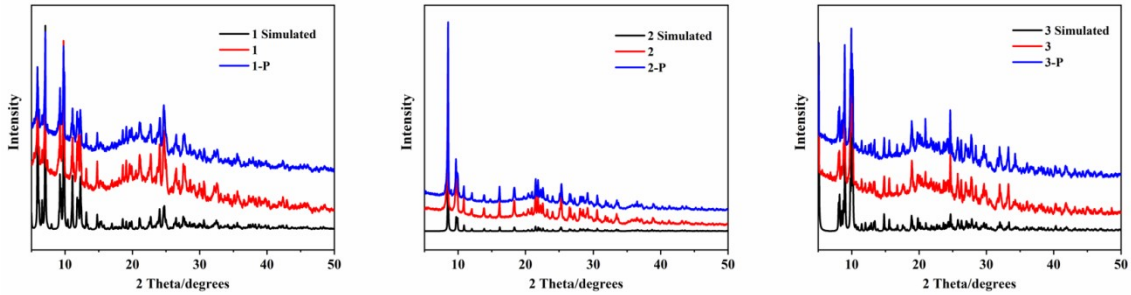

Fig. S9. The simulated and experimental PXRD patterns of **1–3** (before irradiation) and **1**-P, **2**-P, **3**-P (after irradiation).

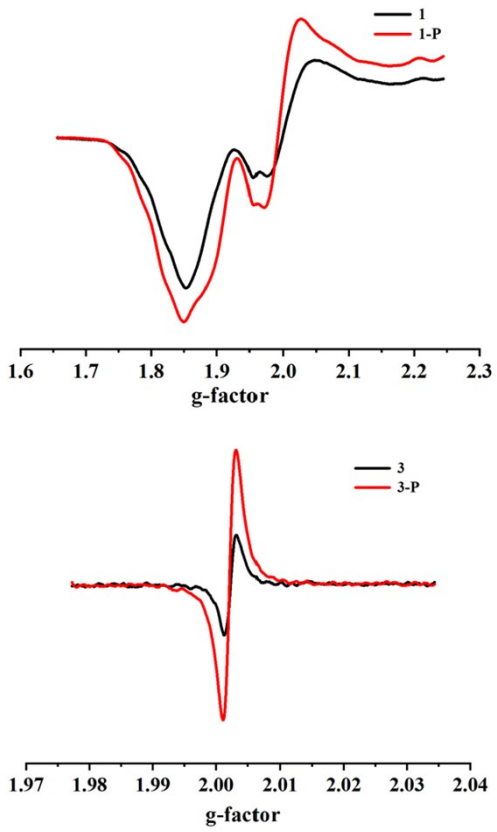

Fig. S10. EPR spectra of **1**, **3** and **1**-P, **3**-P (before and after irradiation).

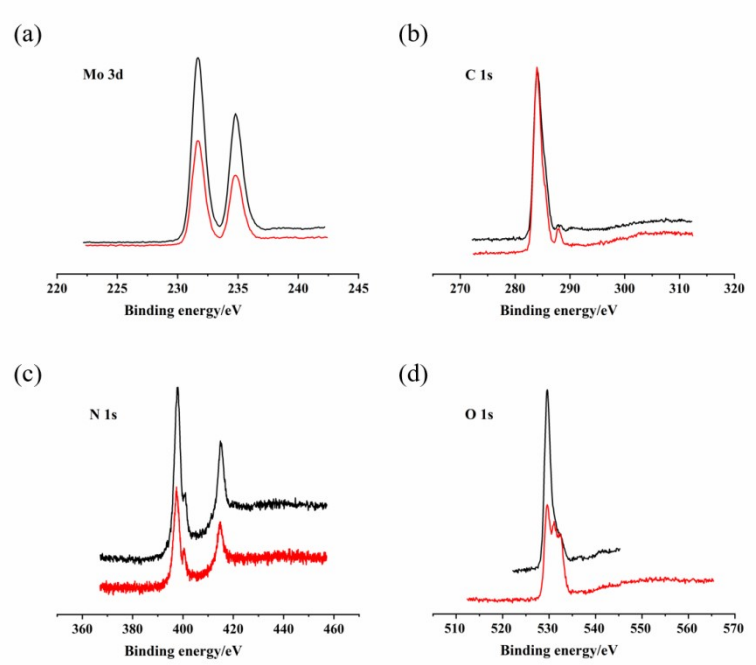

Fig. S11. XPS core-level spectra before (black line) and after (red line) irradiation of **1**.

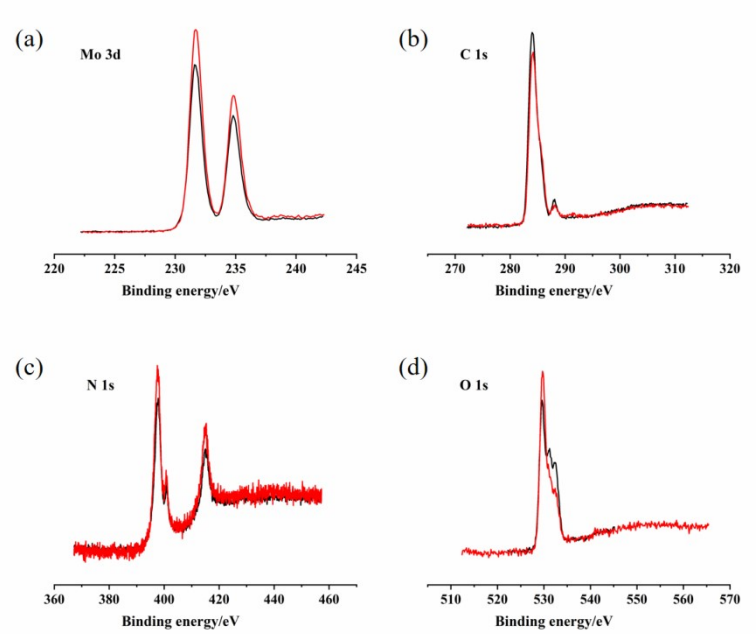

Fig. S12. XPS core-level spectra before (black line) and after (red line) irradiation of **2**.

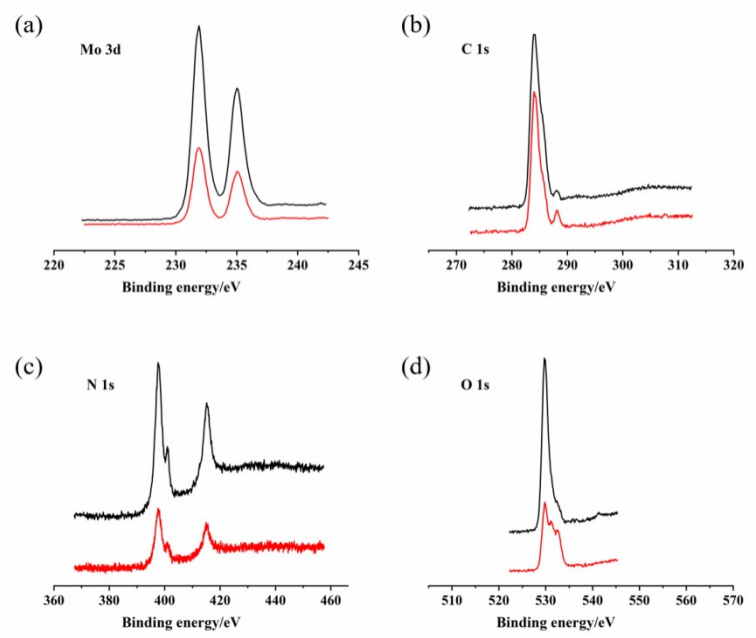

Fig. S13. XPS core-level spectra before (black line) and after (red line) irradiation of **3**.

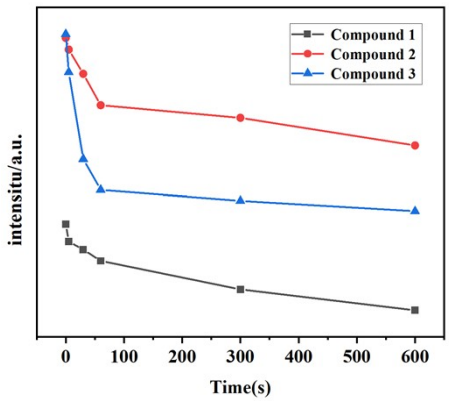

Fig. S14. The plots of fluorescence intensity changes at 400 nm for **1**, 397 nm for **2**, 398 nm for **3** with irradiation time vs. UV irradiance.

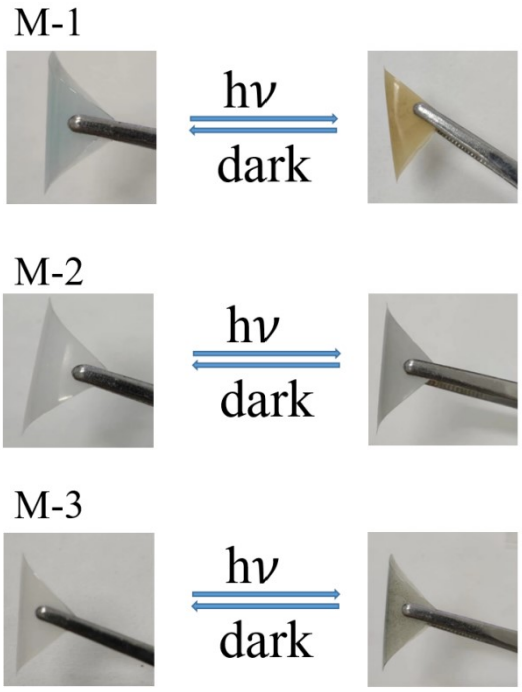

Fig. S15. Flexibility of M-**1**, M-**2** and M-**3** (before and after irradiation).

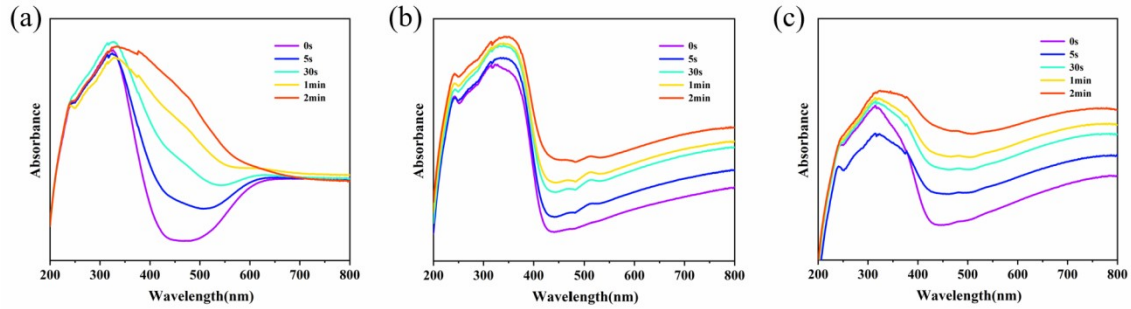

Fig. S16. UV-vis spectral changes of M-**1**, M-**2** and M-**3** (a-c) in the solid state upon UV (200–400 nm) and visible-light illumination (>400 nm) at room temperature in air.

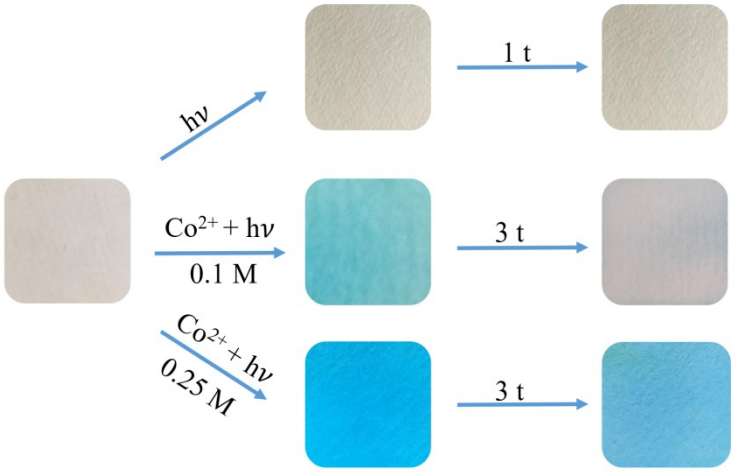

Fig. S17. Color change for visual detection of Co^{2+} by Z-**2** (before and after irradiation).

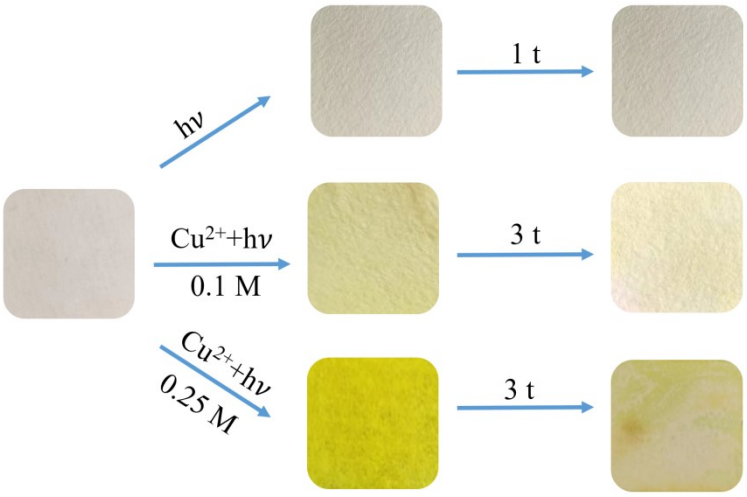

Fig. S18. Color change for visual detection of Cu^{2+} by Z-**2** (before and after irradiation).

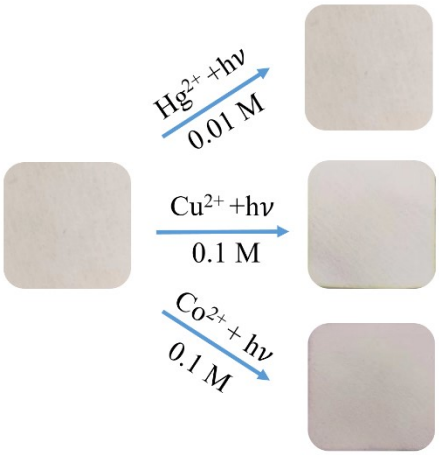

Fig. S19. Blank test paper immersed in solutions containing different ions and irradiated with color changes.

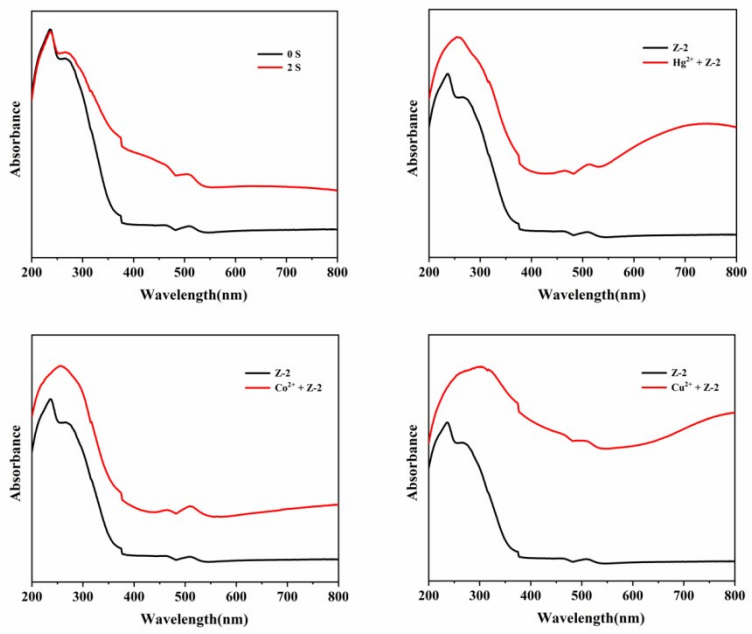

Fig. S20. UV-vis spectral changes of Z-**2**, Z-**2**(Hg^{2+}), Z-**2**(Co^{2+}) and Z-**2**(Cu^{2+}) in the solid state upon UV (200–400 nm) and visible-light illumination (>400 nm) at room temperature in air.

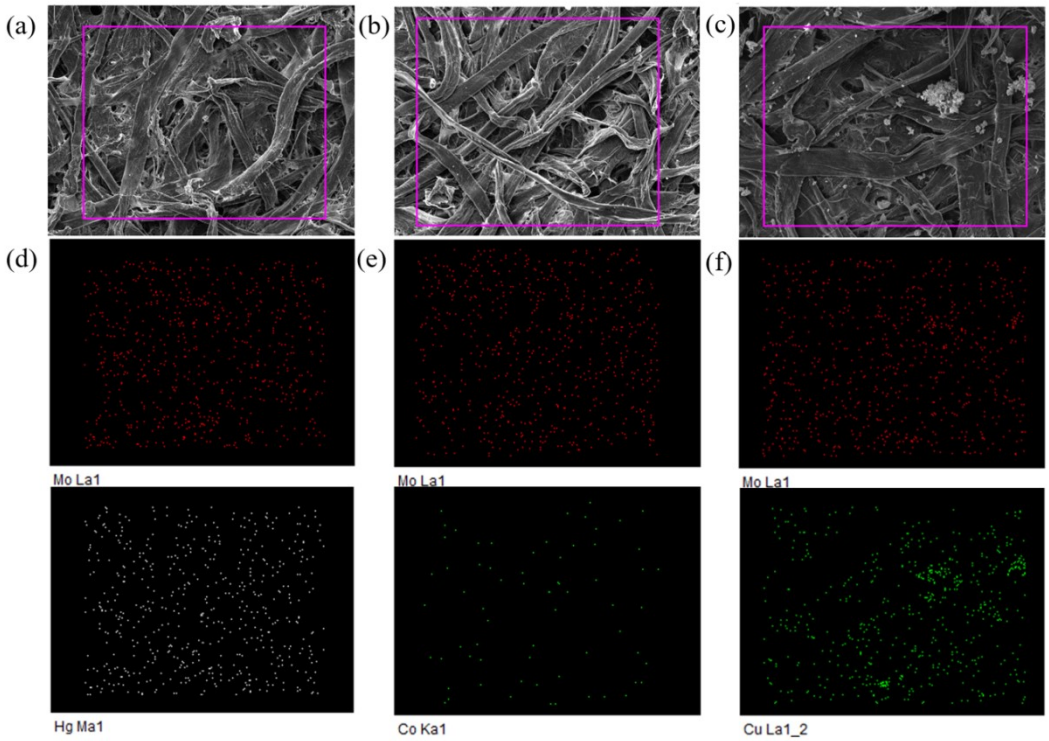

Fig. S21. (a-c) Morphology and structures of Z-**2**(Hg^{2+}), Z-**2**(Co^{2+}) and Z-**2**(Cu^{2+}) characterized by SEM. (d–f) EDS elemental mapping images of Z-**2**(Hg^{2+}), Z-**2**(Co^{2+}) and Z-**2**(Cu^{2+}).

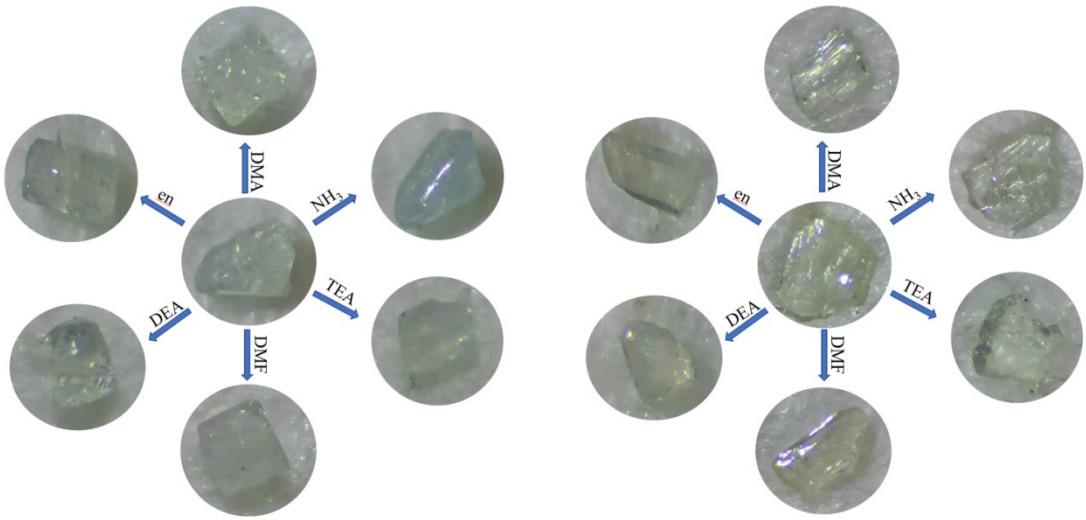

Fig. S22. Color change of **2** and **3** before and after detection of organic amine.

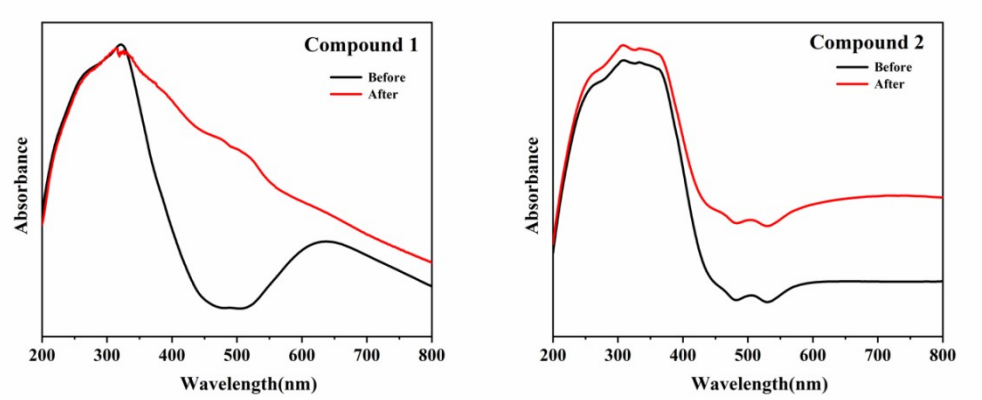

Fig. S23. UV/vis spectra of compounds **1** and **2** before and after exposure to NH_3 vapors.

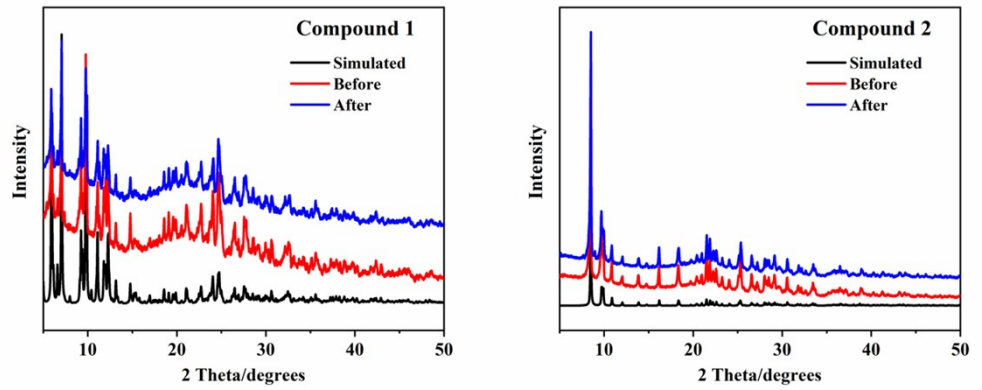

Fig. S24. The simulated and experimental PXRD patterns of **1** and **2** (before and after ammonia detection).

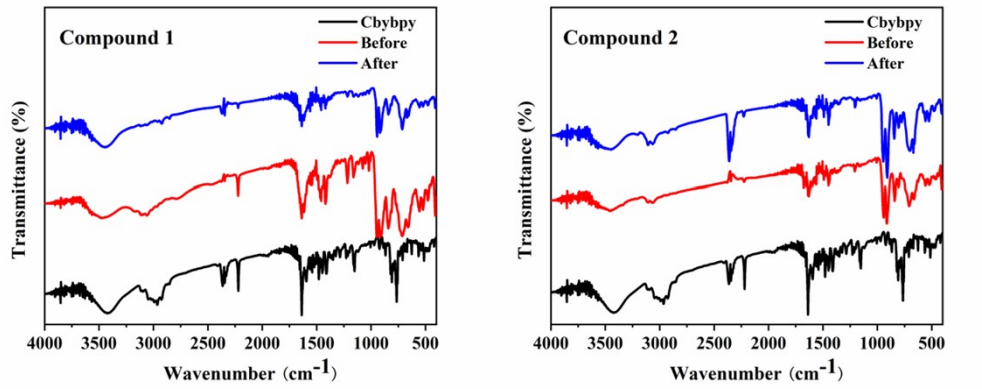

Fig. S25. The IR spectra of Cbybpy, compounds **1** and **2** (after ammonia detection).